File S1. Expanded Materials and Methods

Strain construction

Most of the details of the strain constructions are in Table S1. As in previous studies (for example, Lee *et al.*, 2009), we used derivatives of the sequence-diverged haploids W303-1A and YJM789. These haploids with various genetic alterations were crossed to generate the diploids used to assay genetic instability. Most haploid strains were constructed by transformation with PCR-generated DNA fragments or by sporulating nearly-isogenic diploids. The genotypes of spores for auxotrophic markers were determined by replica-plating spore-derived colonies to omission media. The replacements of genes with drug-resistance markers were confirmed by PCR analysis as described in Tables S2 and S3. Mating type was determined by PCR with primers MATaF, MATalphaF, and MATR (Table S3). *MAT***a** and *MAT*α loci were associated with 500 and 400 bp fragments, respectively.

Measurements of rates of genetic instability induced by loss of RNase H

We used three methods to examine the rates of instability in strains with mutations affecting RNase H activity. We first measured the frequency of genomic alterations in sub-cultured diploid strains of the following genotypes: wild-type, *rnh1*Δ, *rnh201*Δ, *rnh1*Δ *rnh201*Δ, *pol2-M644L*, and *rnh201*Δ *pol2-M644L*. All diploids were generated by crossing haploids isogenic with W303-1A and YJM789. Two independently-derived isolates from each strain were streaked with a toothpick to single colony density on rich growth medium (YPD) for the first subculture. For the second subculture, five-ten colonies from each isolate were then re-streaked to YPD. One colony derived from each of these ten to twenty colonies was then re-streaked again. For the mutant backgrounds, this procedure was repeated twenty times. For the wild-type, only ten sub-culturings

were performed. All sub-culturing experiments were done at 30^0 C. Following sub-culturing, the passaged strains were examined by whole-genome microarrays as described below.

The second method of measuring genome stability was to monitor the frequency of formation of red/white sectored colonies in strains in which the *ADE2* gene was inserted near the right telomere of one copy of chromosome IV and the *K. lactis URA3* was inserted at the allelic position on the other copy (Fig. 3). The homologs with the *ADE2* and *URA3* genes had wild-type and mutant alleles of the centromere-linked *TRP1* gene, respectively. Experiments were initiated using colonies formed on YPD plates. For each genotype, we used one colony from two independently-constructed diploids. Each colony was suspended in water, and diluted to a concentration that resulted in about 1000 cells per plate on the diagnostic medium (SD-arginine with 10 micrograms/ml adenine). After three days of growth, we scored plates for red/white sectors using a dissecting microscope. Cells from each sector were then re-streaked to YPD plates and, after two days of growth, the resulting colonies were replica-plated to media lacking uracil or tryptophan. If all of the colonies purified from the white sector were Ura^-, the sectored colony was classified as resulting from a reciprocal crossover (Fig. 3A). If all colonies derived from the white sector were Ura^+, the strain was classified as resulting from BIR (Fig. 3B). White sectors that had mixtures of Ura^+ and Ura^- colonies were not used in our analysis; such sectored colonies could reflect events that occurred subsequent to the first division. Sectored colonies could also result from chromosome loss. In such colonies, the red sector would be Trp^-. Of 173 red/white sectored colonies, only one example of chromosome loss was observed.

The assay of genome instability based on red/white colony formation has the unfortunate characteristic of being non-selective. For the third assay, we selected for loss of the heterozygous *URA3* gene located near the right telomere by plating cells on

medium containing 5-fluoro-orotate (5-FOA). For this assay, we suspended colonies of each strain in 1 ml of water, and plated about 100 microliters of each undiluted suspension on medium containing 5-FOA (1 mg/ml), and a dilution of the suspension on non-selective medium (SD-complete medium). Between 15 and 25 colonies were examined for each genotype. From measurements of the number of 5-FOA^R colonies and the total number of cells in each colony/culture, we calculated the rate of 5-FOA^R using the method of the median (Lea and Coulson, 1949). To obtain the 95% confidence intervals for the rate estimates, we used Table B11 in Altman (1990).

Microarray analysis

DNA samples for microarray analysis were prepared by methods similar to those described in St. Charles *et al.* (2012). In brief, yeast cells were grown to stationary phase in liquid YPD cultures (5-15 ml). Cells were harvested by centrifugation, and the resulting cell pellet was resuspended in about 500 microliters of 42^0 molten agarose (0.5% low-melt agarose in 100 mM EDTA); 20 microliters of a 25 mg/ml solution of Zymolyase was then added. This mixture was distributed among about seven plug molds, each containing about 100 microliters. The samples were allowed to solidify at 4°C for 30 minutes. After solidifying, the plugs were suspended in 1ml of 10mM Tris/500mM EDTA (TE buffer), and incubated in a 15 ml tube at 37°C for at least 10 hours. 100 microliters of a 5% sarcosyl, 5 mg/ml proteinase-K in 500mM of EDTA (pH7.5) solution was then added to each sample, and the samples were incubated at 50° C for at least 12 hours. Each plug was then washed twice with TE buffer. The second incubation was performed with shaking at 4° C for at least 12 hours. After 12 hours, we did a third wash at 4^0 with TE buffer.

DNA was then extracted from four plugs of each sample using methods described in St. Charles *et al.* (2012). The samples were sonicated to yield DNA fragments of about 250 bp. The samples derived from each plug were pooled for labeling with fluorescent dyes. Each sample had about 100 micrograms/ml of DNA, and about 10 microliters was used in the labeling reactions.

For our method of analysis, the hybridization of DNA derived from experimental strains with LOH events was performed in competition with DNA from control strains heterozygous for all SNPs. The experimental strains were labeled with Cy3-dUTP, whereas the control strain was labeled with Cy5-dUTP (details in St. Charles *et al.*, 2012). The labeled nucleotides were provided as part of the Invitrogen Bioprime Array CGH Genome Labeling Module. The control and experimental labeled samples were combined, and hybridized to the microarrays. Two types of custom-made Agilent microarrays were used, one to analyze LOH events throughout the genome (St. Charles *et al.*, 2012) and one to examine LOH events on the right arm of chromosome IV (St. Charles and Petes, 2013). The sequences and locations of oligonucleotides on the whole-genome array are in Table S5 (St. Charles *et al.*, 2012), and the sequences and locations of oligonucleotides on the chromosome IV-specific array are in Table S9 (St. Charles and Petes, 2013).

After hybridization (conditions described in St. Charles *et al.*, 2012), the arrays were scanned using the GenePix scanner and GenePix Pro 6.1 software. A GenePix Results (.gpr) file was generated for each sample using the Batch Analysis feature in Gene Pix Pro 6.1. This file contains a “ratio of medians (635 nm/532 nm)” for each oligonucleotide represented on the microarray. This ratio reflects the fluorescence of the Cy5-labeled experimental sample relative to the Cy3-labeled control. Each SNP analyzed was represented by at least four 25-base oligonucleotides, two identical to the Watson and Crick strands containing the W303-1A allele and two identical to the Watson and Crick

strands of the YJM789 allele. We used programs written in Perl and R to automate the analysis and to plot hybridization levels throughout the genome (programs available on request). The resulting plots were done at two levels of resolution. Low-resolution plots depicted hybridization ratios that are the moving average of ten adjacent SNPs, whereas high-resolution plots show the ratio of medians at each individual SNP. We eliminated from the analysis any oligonucleotides that were "flagged" by the GenePix Pro 6.1 software or that had a level of fluorescence that was in the bottom 5% of intensities in both the 635 nm and 532 nm channels.

Following normalization, the hybridization ratios of heterozygous SNPs for the experimental samples were about 1 to both the W303-1A- and YJM789-related SNPs. For LOH regions in which W303-1A-related SNPs were homozygous, the ratio of hybridization to these SNPs was about 1.5 and the ratio of hybridization to YJM789-related SNPs was about 0.2. For LOH regions in which YJM789-related SNPs became homozygous, these ratios were reversed.

Microarray slides were re-used about six times by stripping the slides of the labeled DNA. Microarray slides containing DNA probes were stripped by placing them in stripping buffer (10 mM potassium phosphate, pH 6.6), and slowly heating to them to the boiling point over about one hour. After rinsing in water, the slides were stored in a nitrogen-containing cabinet. The slides that cover the microarray slides (gasket slides) were boiled in the stripping buffer for 40 minutes, rinsed in water, and dried by centrifugation. Following stripping, we usually allowed the slides to dry for two days before they were used again.

Associating genomic elements with LOH transitions in sub-cultured strains

One of the main goals of this research was to find out whether the LOH events resulting from loss of RNase H were enriched at the locations of specific genomic

elements. The rationale for our analysis is that the breakpoints associated with LOH events should be located near the site of the recombinogenic lesion. In our analysis, we examined only events in which at least two or more adjacent SNPs underwent LOH. To determine the likely "window" containing the recombination initiation site, we used the same procedure employed in our previous studies (for example, St. Charles and Petes, 2013). For interstitial LOH events, we used an association window that included all sequences located between the heterozygous SNPs that most closely flanked the LOH region. For terminal LOH events, the association window was 10 kb centromere-proximal and 10 kb centromere-distal from the homozygous SNP that was closest to the LOH event. Some events were found in most or all of the sub-cultured strains derived from a single isolate. Since these events (marked "redundant" in Table S5) were likely generated in the isolate before sub-culturing, we included redundant events in each category as single events.

We next determined whether specific genetic elements were over-represented in the association windows of different mutant strains. This analysis involved multiple steps. First, for each genotype, we summed the number of bases in the association windows over all of the individual sub-cultured isolates. For example, for the nineteen sub-cultured isolates of the *rnh201* strain about 1.35 Mb were included in the association windows (Table S5). The yeast nuclear genome as annotated in SGD, which includes only two of the approximately 150 rRNA gene repeats, is about 12.1 Mb. As discussed in the legend to Table S10, our microarrays cover about 11.6 Mb of the genome, since these arrays do not include the repetitive sub-telomeric sequences. Thus, the total amount of DNA represented on the arrays for 19 isolates is about 220.4 Mb. The amount of genomic DNA that is not present in the association windows is, therefore, 220.4 Mb – 1.35 Mb or about 219 Mb. Second, we determined the total number of specific genomic elements represented on the array. For example, there are 352 ARS elements in the

genome and 317 ARS elements represented on the array (Table S10). If these elements are placed randomly with respect to the association windows, we expect 37 ARS elements within the association windows: 317 x (1.35 Mb/220.4 Mb) x 19. The expected number of ARS elements located outside of the association windows is 5986: (317 x 19) – 37. We then counted the number of ARS elements within the association windows, determining that there were 31; the observed number of these elements outside of the association windows was 5992. Finally, we compared the observed and expected numbers by Chi-square analysis (Table S11), finding a p value (0.362) that indicates no significant association between LOH breakpoints and ARS elements. We repeated this analysis with twenty other genomic features (described below). After correction of the p values for multiple comparisons (Benjamini and Hochberg, 1995), none of these values were significant.

The numbers and locations of each genomic element tested were assembled from a variety of sources. Ty elements, solo LTR elements, centromeres, intron-containing genes, ARS elements, and tRNA genes were extracted from the S288c reference genome using the YeastMine tool on SGD (Engel *et al.* 2013, genome version R64-1-1; http://www.yeastgenome.org/help/video-tutorials/yeastmine). We also used YeastMine to determine the locations of the genes that were among the top 5% in length ("long gene" category in Tables S10 and S11). The same tool was used to identify the genes with the highest (top 5%) and lowest (bottom 5%) rates of transcription. From the sequence of the ORFs, we calculated the percentage of G bases on the non-transcribed strand. 41 ORFs with ≥ 29% G were identified and used in the association analysis. In addition, we identified 115 ORFs that had a GC-content ≥ 50%; these genes were also used in our analysis (Table S11).

Most of the other references for the locations of various genomic elements are in Table S9. Regions with converging replication forks (TER sites) were described in Table

S2 of Fachinetti *et al*. (2010). In the same paper, binding sites for the Rbp3p subunit of RNA polymerase II were mapped by chromatin immunoprecipitation followed by microarray analysis. We downloaded these data (GSM409326 on GEO, GSM409326_Rpb3_signal.bar.gz) and converted them to a .txt file. All sites with a normalized log2 value less than 0.4 were eliminated from analysis. Adjacent sites less than 1 kb apart were collapsed into single intervals, and the signal was averaged over all collapsed sites. There were 933 such intervals. As sorted by the hybridization values, we used the top 10% (93) of the intervals for our association analysis. 58 of the 71 genomic TER sites were associated with Rpb3p binding (Table S4; Fachinetti *et al.*, 2010). These sites were designated "TER sites related to high transcription" in Tables S9-S12. We also examined the association of LOH breakpoints with sites enriched for the binding of Rrm3p, a helicase involved in promoting replication through certain hard-to-replicate sequences; the map locations of these sites are in Supplemental Table 7 of Azvolinsky *et al.* (2009).

Palindromic sequences greater than 16 bp were examined using data from Lisnic *et al.* (2005), and sequences likely to form G4 quadruplex structures were obtained from Dataset S1 of Capra *et al*. (2010). Hershman *et al.* (2008) examined differential expression of genes by *S. cerevisiae* in response to N-methyl mesoporphyrin IX (NMM), a drug that stabilizes G4 quadruplexes *in vitro*. We examined the association of genes whose transcription was significantly ($p<0.001$) altered by the drug (Supplementary Table 5 of Hershman *et al.*, 2008) with the LOH events. We also examined associations with genomic regions with high levels of Elc1p, a protein involved in resolving conflicts between converging transcripts (Hobson *et al.*, 2012). The top 10% of Elc1p-binding sites (Table S1 of Hobson *et al*., 2012) were used to look for associations. The locations of RNA/DNA hybrids in *rnh1Δ rnh201Δ* strains have been recently mapped (Chan *et al.*, 2014). We examined the association of those sites that were at least ten-fold enriched

(Dataset S7 of Chan *et al.*, 2014) with our LOH data. Lastly, based on observations of a non-random association of R-loops and poly A tracts (Doug Koshland, University of California, Berkeley), we identified all uninterrupted poly A or poly T tracts that were at least 25 bases in length. We examined the association of these 41 tracts with LOH events. As described in the main text, after correction for multiple comparisons, none of the genomic elements that we examined were significantly associated with the LOH events in sub-cultured strains.

In our analysis, any elements that are within the association windows or that span the association windows are included in our analysis. For most of the genomic elements examined, the size of the element was small, less than 10% of the average size of the association window. For four of the elements (Ty elements, TER sites, TER sites associated with high levels of transcription, and "Long Genes"), however, the size of the element was greater than 10% of the size of the association window. For these comparisons, we expanded all association windows by an amount equivalent to the average size of the element. For example, when we examined the associations between Ty elements and LOH events, the association windows were expanded by 6 kb, the size of a Ty element.

Associating genomic elements with LOH transitions in sectored colonies

In sectored colonies (reflecting crossovers on the right arm of chromosome IV), the borders of the association window were the coordinates of the heterozygous SNP closest to the most centromere-proximal LOH transition and the homozygous SNP closest to the most centromere-distal LOH transition (Table S8). All association windows were used in our analysis. The right arm of chromosome IV represents about 1.4 Mb, and the number of genomic elements on the right arm of IV are given in Table S10. Our methods of calculating significant associations between genomic elements and LOH

events are chromosome IV were analogous to those described for the sub-cultured strains. We performed microarray analysis on sectored colonies of only two genotypes: *rnh201*Δ and *rnh1*Δ *rnh201*Δ. No significant associations were found between LOH events in these strains and any of the tested genomic elements (Table S12).

Regions of apparent terminal duplications/deletions at repetitive sub-telomeric regions

By microarray analysis, regions of LOH are unambiguous since the hybridization signals for one set of allelic SNPs increases for the same genomic region in which the other set of allelic SNPs decreases. From previous studies (Y. Yin and T. Petes, unpublished observations), we have found a small number of apparent terminal duplications and deletions that likely reflect LOH events on non-homologous chromosomes with shared sub-telomeric sequences. In the current study, we observed several such events among the sub-cultured strains as described below.

KO_244_1_XX_D (*rnh201*Δ *pol2-M644L*). In this isolate, we observe a terminal LOH event (YJM789-derived SNPs becoming homozygous) on chromosome X (transition coordinates 708414-728414). This strain also has a terminal deletion on the left arm of chromosome IV (transition coordinates 15561-18870), resulting in loss of W303-1A-derived sequences. In the sequence of S288c (nearly isogenic with W303-1A), we found that the chromosome X sequences between 730-742 kb are almost identical to the region 3-15 kb on chromosome IV. For example, the oligonucleotide 5211 (Table S3 in St. Charles *et al.,* 2012), near the right telomere of IV is repeated near the right telomere of X. Thus, an LOH event causing loss of W303-1A-derived SNPs from chromosome X will appear as a reduced signal of hybridization to W303-1A-specific SNPs near the right telomere of chromosome IV. It is unclear whether the YJM789-derived copy of chromosome X has the same duplication as the W303-1A-derived homolog. When sequences from a portion of the repeated region on chromosome IV (10 kb to 12 kb) are

used in a BLAST search of the YJM789 database in SGD, the sequences match to chromosome IV contigs without matching to chromosome X contigs. Finally, we note that LOH events that involve the left end of IV will not have a detectable effect on the microarray pattern observed on the right end of chromosome X because the most centromere-distal oligonucleotide on the array is at position 727 kb which is centromere-proximal to the repeated sequences.

KO_5_6_E (*rnh1*Δ *rnh201*Δ); KO_5_9_H (*rnh1*Δ *rnh201*Δ); KO_75_2_XX_H (*rnh201*Δ). These three strains had an apparent terminal deletion on chromosome VI, resulting in loss of YJM789-derived sequences. The coordinates for the deletions were similar in all three isolates beginning near coordinate 30,000 kb and proceeding to the telomere. All three strains also had terminal LOH events on chromosome X, resulting in loss of YJM789-derived SNPs and duplication of W303-1A-derived SNPs. The breakpoints of these LOH events were different in the three strains: KO_5_6_E (about 135 kb); KO_5_9_H (about 127 kb); KO_75_2_XX_H (about 36 kb). According to Wei *et al.* (2007), in YJM789, an approximately 30 kb segment derived from the left end of chromosome VI is translocated to the left end of chromosome X. From these data, the W303-1A SNPs are at the right end of chromosome VI, whereas the YJM789 SNPs are at the right end of chromosome X. Since sub-telomeric repeats are difficult to assemble, it is also possible that YJM789 has two copies of the 30 kb segment, one on VI and one on X. An LOH event on the left arm of chromosome X in which YJM789-derived sequences are lost will result in an apparent deletion of YJM789-specific sequences near the left telomere of VI. It should also be noted that there are only eight SNPs on the microarray from the 30 kb segment.

KO_75_2_XX_I (*rnh201*Δ); KO_5_9_I (*rnh1*Δ *rnh201*Δ). These strains both contain apparent terminal duplications of YJM789-derived sequences on the left arm of

chromosome XV with the starting point of the duplication near coordinate 22 kb. Both strains have terminal LOH events on the left end of chromosome IX, resulting in duplication of YJM789-derived SNPs and loss of W303-1A-derived SNPs. The breakpoints for the LOH event are near coordinate 105 kb for KO_75_2_XX_I and near coordinate 336 for KO_5_9_I. The sub-telomeric regions of chromosomes IX and XV share considerable homology in both the YJM789 and W303-1A/S288c genomes. In the S288c genomes, sequences from chromosome XV with coordinates about 22-31 kb share extensive homology with sequences from chromosome IX located between coordinates 17-26 kb. However, according the SGD database and our analysis, the oligonucleotides that have an elevated signal on chromosome XV are not in the region of the genome that is repeated on chromosome IX in either the W303-1A or the YJM789 genomes. For example, in isolate KO_75_2_XX_I, the YJM789-specific oligonucleotide at position 22005 clearly has an elevated level of hybridization. The sequence of this oligonucleotide, however, is not present on chromosome IX. Similarly, in isolate KO_5_9_I, the level of hybridization to the YJM789-specific oligonucleotide 19925 is elevated, although the sequence of this oligonucleotide is not on chromosome IX.

Although we do not have a definitive explanation of these observations, one possibility is that the YJM789 isolate used in our studies has a derivative of chromosome IX in which the terminal 22 kb of chromosome X replaces the terminal 16 kb of chromosome IX. Such a derivative could be formed as a consequence of a break-induced replication event in which a broken end of the YJM789-derived copy of chromosome IX duplicates a portion of the YJM789-derived chromosome XV homolog. The initiation point of this invasion would be in the region of shared homology. In diploid strains with this derivative, an LOH event on chromosome IX, occurring centromere-proximal to the duplicated region, would duplicate both YJM789-related SNPs on chromosome XV and cause a duplication of YJM789-derived sequences from the

terminal region of chromosome XV. It should be noted that an LOH event on chromosome XV that results in LOH for the terminal repeated sequences would not be annotated as an LOH event on chromosome IX since the first oligonucleotide used to diagnose LOH for chromosome IX is located at coordinate 25 kb. Although this model is consistent with our observations, our observations could also reflect an assembly error of the genomic sequences.

KO_5_6_K (*rnh1*Δ *rnh201*Δ). In this isolate, there is an apparent duplication of YJM789-derived sequences on the left arm of chromosome XVI with a transition point between coordinates 23222 and 26225. There were also terminal LOH events on several chromosome arms including the right arm of chromosome XIII, duplicating YJM789-derived SNPs; the LOH event on XV has a transition between coordinates 889 and 892 kb. The left arm of chromosome XVI (25.8-26.4 kb) shares homology with the right arm of chromosome XIII (coordinates 917.5 kb to 917.8 kb), although the oligonucleotides that have increased levels of hybridization on chromosome XVI in KO_5_6_K are not annotated as duplicated on any other homolog. One explanation of the data is that a break within the shared homology occurred on chromosome XIII that was repaired by a BIR event involving chromosome XVI. A subsequent LOH event on XIII could result in the observed apparent duplication of XVI sequences as well as the terminal LOH event duplicating YJM789-derived SNPs. Alternatively, there may be an incorrect assembly or annotation of the sub-telomeric sequences in the databases.

KO_5_9_D (*rnh1*Δ *rnh201*Δ). In this isolate, there is an apparent deletion of W303-1A-derived sequences on the right arm of chromosome I with a transition point between coordinates 195120 and 203572. There is also a terminal LOH event on the right arm of chromosome VIII, resulting in loss of W303-1A-derived sequences, with a transition point between 199775 and 207066. In the S288c genome, there is a large region of conserved

homology that includes the coordinates 207-227 kb on the right end of chromosome I and coordinates 528-556 kb on the right end of VIII. Several of the SNPs located near the right end of chromosome I (for example, oligonucleotide 208214; Table S3, St. Charles *et al.*, 2012) are duplicated on the right end of VIII. Therefore, an LOH event that causes loss of W303-1A-derived SNPs and duplication of YJM789-derived SNPs will result in an apparent deletion of W303-1A sequences from the right end of chromosome I.

Supplemental Figure Legends

Figure S1. Patterns of LOH in sub-cultured strains. Each line represents markers in a diploid isolate. Green indicates heterozygous SNPs; red, homozygous W303-1A-derived SNPs; black, homozygous YJM789-derived SNPs. The yellow circle shows the centromere. Each transition between heterozygous and homozygous SNPs or between two regions with different homozygous SNPs is labeled with a lower case letter. Classes a1-a4 are simple terminal LOH events. In Classes a6-a8, the two transitions (one marked with an asterisk) are separated by distances that are two standard deviations longer than the median length of a mitotic conversion tract. The two transitions are, therefore, likely to reflect two different recombination events. Classes b1 and b2 represent simple interstitial LOH events (gene conversions), whereas in Classes b3-b5, the conversion event is interrupted by a region of heterozygosity. Classes f1-f12 represent terminal LOH events with complex patterns of associated LOH events. Only Classes a1-a4, b1, and b2 were used for our association studies.

Figure S2. Deletions and duplications in sub-cultured strains. This diagram shows the patterns of deletions and duplications in diploid isolates. As in Fig. S1, the green line indicates heterozygous SNPs, and yellow circles show the centromere. The deletion or duplication is shown as a line that is half as wide as the green lines. The Classes dd9 and dd10 show interstitial duplications of W303-1A-derived and YJM789-derived SNPs, respectively. The Class dd12 shows an interstitial deletion in which W303-1A-derived SNPs were removed. The coordinates for the transitions are in Table S6.

Figure S3. Aneuploidy events in sub-cultured strains. Trisomic, but not monosomic, aneuploid events were observed in our studies. For each chromosome, we indicate whether the strain has W303-1A-derived SNPs (red) or YJM789-derived SNPs (black). Note that many of these aneuploid events are associated with recombination on one or more chromosomes.

Figure S4. Locations of LOH events in the sub-cultured *rnh201Δ* strain. Each of the sixteen chromosomes is shown as a thin black horizontal line with SNPs shown as very short vertical yellow lines. The centromeres are represented by black ovals. Red and blue bars show regions of interstitial LOH in which the W303-1A-derived SNPs became homozygous and the YJM789-derived SNPs became homozygous, respectively. Black arrows indicate the positions of terminal LOH events that were unassociated with a gene conversion event. Red arrows and blue arrows indicate terminal LOH events that were associated with a conversion that made W303-1A-derived SNPs and YJM789-derived SNPs homozygous, respectively. Triangles indicate deletions (red for a deletion of W303-1A-derived sequences and blue for a deletion of YJM789-derived sequences) and inverted triangles indicate duplications (same color code as for deletions).

Figure S5. Location of LOH events in the sub-cultured *rnh1Δ rnh201Δ* strain. The mapped events are shown with the same code as in Fig. S4.

Figure S6. Location of LOH events in the sub-cultured *rnh201Δ pol2-M644L* strain. The mapped events are shown with the same code as in Fig. S4.

Figure S7. Patterns of LOH in sectored colonies. In this depiction, each sectored colony is represented by a pair of lines with the red sector shown as the top line. We use the same color code for heterozygous and homozygous regions as in Fig. S1. Other features of these patterns are described in the main text.

Supplemental Tables.

Table S1. Strain list.

Table S2. Plasmid list.

Table S3. Primers list.

Table S4. Strains used in different assays of LOH.

Table S5. LOH events in sub-cultured strains.

Table S6. Deletion/duplication events in sub-cultured strains.

Table S7. Trisomy events in sub-cultured strains.

Table S8. LOH events on chromosome IV in sectored colonies.

Table S9. References used to determine the locations of genomic elements.

Table S10. Number of genomic elements represented on the microarrays.

Table S11. Association of LOH events in sub-cultured strains with various genomic elements.

Table S12. Association of LOH events in sectored colonies with various genomic elements on the right arm of chromosome IV.

References

Altman, D. G. (1990) *Practical Statistics for Medical Research*. (Chapman and Hall/CRC Texts in Statistical Science).

Aksenova, A.Y, P.W. Greenwell, M. Dominska, A.A. Shishkin, J.C. Kim, T.D. Petes, and S.M. Mirkin (2013) Genome rearrangements caused by interstitial telomeric sequences in yeast. *Proc Natl Acad Sci USA* 110(49): 19866-19871.

Azvolinsky, A., P.G. Giresi, J.D. Lieb, and V.A. Zakian (2009) Highly transcribed RNA polymerase II genes are impediments to replication fork progression in *Saccharomyces cerevisiae*. Mol Cell 34: 722-34.

Benjamini Y. and Y. Hochberg (1995) Controlling the false discovery rate: A practical and powerful approach to multiple testing. *J Roy Stat Soc A Sta* 57(1): 289-300.

Capra, J.A., K. Paeschke, M. Singh, V.A. Zakian (2010) G-quadruplex DNA sequences are evolutionarily conserved and associated with distinct genomic features in*Saccharomyces cerevisiae*. *PLoS Comput Biol* 6: e1000861

Chan, Y. A., M.J. Aristizabal, Y.T. Lu Phoebe, Z. Luo, A. Hamza, M.S. Kobor, P.C. Stirling, P. Hieter (2014) Genome-wide profiling of yeast DNA:RNA hybrid prone sites with DRIP-Chip. *PLoS Genet* 10(4): e1004288.

Engel S.R., F.S. Dietrich, D.G. Fisk, G. Binkley, R. Balakrishnan, M.C. Costanzo, S.S. Dwight, B.C. Hitz, K. Karra, R.S. Nash, S. Weng, E.D. Wong, P. Lloyd, M.S. Skrzypek, S.R. Miyasato, M. Simison, J.M. Cherry (2013) The Reference Genome Sequence of Saccharomyces cerevisiae: Then and Now. *G3* pii: g3.113.008995v1. doi: 10.1534/g3.113.008995.

Fachinetti, D., R. Bermejo, A. Cocito, S. Minardi, Y. Katou, Y. Kanoh, K. Shirahige, A. Azvolinsky, V.A. Zakian, M. Foiani (2010) Replication termination at eukaryotic

chromosomes is mediated by Top2 and occurs at genomic loci containing pause elements. *Molecular Cell*. 39(4): 595-605.

Goldstein, A.L., and J.H. McCusker (1999) Three new dominant drug resistance cassettes for gene disruption in Saccharomyces cerevisiae. *Yeast* 15(14): 1541-1553.

Gueldener, U., J. Heinisch, G.J. Koehler, D. Voss, and J.H. Hegemann (2002) A second set of loxP marker cassettes for Cre-mediated multiple gene knockouts in budding yeast. *Nucleic Acids Res* 30(6): e23.

Hershman, S.G., Q. Chen, J.Y. Lee, M.L. Kozak, P. Yue, L.S. Wang, and F.B. Johnson (2008) Genomic distribution and functional analyses of potential G-quadruplex-forming sequences in *Saccharomyces cerevisiae*. *Nucleic Acids Res* 36(1): 144-156.

Hobson, D. J., W. Wei, L.M. Steinmetz, J.Q. Svejstrup (2012) RNA polymerase II collision interrupts convergent transcription. *Mol Cell* 48(3): 365-374.

Kim, N., J. Cho, Y.C. Li, and S. Jinks-Robertson (2013) RNA:DNA hybrids initiate quasi-palindrome associated mutations in highly transcribed yeast DNA. *PLoS Genet* 9(11): e1003924.

Lea, D.E. and C.A. Coulson (1949) The distribution of number of mutants in a bacterial population. *J Genet* 49: 264-285.

Lee, P.S., P.W. Greenwell, M. Dominska, M. Gawel, M. Hamilton, and T.D. Petes (2009) A fine-structure map of spontaneous mitotic crossovers in the yeast *Saccharomyces cerevisiae*. *PLoS Genet* 5(3): e1000410.

Lisnic, B., I.K. Svetec, H. Saric, I. Nikolic, and Z. Zgaga (2005) Palindrome content of the yeast *Saccharomyces cerevisiae* genome. *Curr Genet* 47: 289-297.

Longtine, M.S., A. McKenzie III, D.J. Demarini, N.G. Shah, A. Wach, A. Brachat, P. Philippsen, and J.R. Pringle (1998) Additional modules for versatile and economical

PCR-based gene deletion and modification in *Saccharomyces cerevisiae*. *Yeast* 14: 953-961.

Mortimer, R.K. and J.R. Johnston (1986) Genealogy of principal strains of the yeast genetic stock center. *Genetics* 113(1): 35-43.

Nick McElhinny, S.A., D. Kumar, A.B. Clark, D.L. Watt, B.E. Watts, E.B. Lundström, E. Johansson, A. Chabes, and T.A. Kunkel (2010) Genome instability due to ribonucleotide incorporation into DNA. *Nat Chem Biol* 6(10): 774-781.

Song, W., M. Dominska, P.W. Greenwell, and T.D. Petes (2014) Genome-wide high-resolution mapping of chromosome fragile sites in *Saccharomyces cerevisiae*. *Proc Natl Acad Sci USA* 111(21): e2210-e2218.

St. Charles, J., E. Hazkani-Covo, Y. Yin, S.L. Andersen, F.S. Dietrich, P.W. Greenwell, E. Malc, P. Mieczkowski, and T.D. Petes (2012) High-resolution genome-wide analysis of irradiated (UV and γ-rays) diploid yeast cells reveals a high frequency of genomic loss of heterozygosity (LOH) events. *Genetics* 190(4): 1267-1284.

St. Charles, J. and T.D. Petes (2013) High-resolution mapping of spontaneous mitotic recombination hotspots on the 1.1Mb arm of yeast chromosome IV. *PLoS Genet* 9(4): e1003434.

Thomas, B.J. and R. Rothstein (1989) Elevated recombination rates in transcriptionally active DNA. *Cell* 56(4): 619-630.

Vernon, M., K. Lobachev, and T.D. Petes (2008) High rates of “unselected” aneuploidy and chromosome rearrangements in *tel1 mec1* haploid yeast strains. *Genetics* 179(1): 237-247.

Wei, W., J.H. McCusker, R.W. Hyman, T. Jones, Y. Ning, Z. Cao, Z. Gu, D. Bruno, M. Miranda, M. Nguyen, J. Wilhelmy, C. Komp, R. Tamse, X. Wang, P. Jia, P. Luedi, P.J. Oefner, L. David, F.S. Dietrich, Y. Li, R.W. Davis, and L.M. Steinmetz (2007)

Genome sequencing and comparative analysis of *Saccharomyces cerevisiae* strain YJM789. *Proc Natl Acad Sci USA* 104(31): 12825-12830.

Zhao, X., E.G. Muller, and R. Rothstein (1998) A suppressor of two essential checkpoint genes identifies a novel protein that negatively affects dNTP pools. *Mol Cell* 2: 329-340.

Table S1. Strain list

Strain Name	Relevant genotype	Construction or source	Genotype	Strain background
S288c	Wild type	Mortimer and Johnston 1986	*MATα SUC2 gal2 mal2 mel flo1 flo8-1 hap1 ho bio1 bio6*	S288c
W1588-4c	Wild type	Zhao *et al.* 1998	*MAT**a** leu2-3,112 his3-11,15 ura3-1 ade2-1 trp1-1 can1-100 RAD5*	W303-1A
W303-1A	Wild type	Thomas and Rothstein 1989	*MAT**a** leu2-3,112 his3-11,15 ura3-1 ade2-1 trp1-1 can1-100 RAD5*	W303-1A
SMY710	Wild type	Aksenova *et al.* 2013	*MAT**a** leu2-Δ1 trp1-Δ63 ura3-52 his3-200 ade2Δ::kanMX*	S288c
MV70	Wild type	Vernon *et al.* 2008	*MAT**a**/MATα trp1-1/trp1-1 leu2-3,112/leu2-3,112 his3-11,15/his3-11,15 ura3-1/ura3-1 ade2-1/ade2-1 can1-100/CAN1 hom3-10/HOM3 rad5/RAD5 tel1Δ::kanMX/TEL1 mec1-21/MEC1*	W303-1A/ W303-1A
PG308	Wild type	MV70 transformed with PCR fragment amplified from pAG25 using primers Tel1NatF and Tel1NatR.	*MAT**a**/MATα trp1-1/trp1-1 leu2-3,112/leu2-3,112 his3-11,15/his3-11,15 ura3-1/ura3-1 ade2-1/ade2-1 can1-100/CAN1 hom3-10/HOM3 rad5/RAD5 tel1Δ::natMX/TEL1 mec1-21/MEC1*	W303-1A/W303-1A
PG309(2)	Wild type	PG308 transformed with PCR fragment amplified from pFA6-kanMXpGAL(x3HA) using primers MRC1pgalF and MRC1pgalR	*MAT**a**/MATα trp1-1/trp1-1 leu2-3,112/leu2-3,112 his3-11,15/his3-11,15 ura3-1/ura3-1 ade2-1/ade2-1 can1-100/CAN1 hom3-10/HOM3 rad5/RAD5 tel1Δ::nat/TEL1 mec1-21/MEC1 MRC1/pGAL-MRC1-kanMX*	W303-1A/ W303-1A
PG309(2)-4a	*tel1*Δ	Spore from PG309(2)	*MATα RAD5 leu2-3,112 his3-11,15 trp1-1 ade2-1 tel1Δ::natMX*	W303-1A
JSC19-1	Wild type	St. Charles and Petes 2013	*MATα ade2-1 ura3 gal2 ho::hisG can1Δ::natMX*	YJM789
JSC21-1	Wild type	St. Charles and Petes 2013	*MATα ura3 gal2 ho::hisG ade2-1 can1Δ::natMX IV1510386::SUP4-o*	YJM789
JSC12	Wild type	St. Charles and Petes 2013	*MAT**a** leu2-3,112 his3-11,15 ura3-1 ade2-1 trp1-1 can1Δ::natMX RAD5 IV1510386::kanMX-can1-100*	W303-1A
SJR3585	Wild type	Spore from diploid PG309(2)-4a x JSC12	*MAT**a** RAD5 leu2-3,112 trp1-1 his3-11,15 ura3-1 ade2-1 IV1510386::kanMX-can1-100*	W303-1A
SJR3615-4	*rnh201*Δ	SJR3585 transformed with PCR fragment amplified from pSR955 using primers	*MAT**a** leu2-3,112 his3-11,15 trp1-1 ura3-1 ade2-1 RAD5 rnh201Δ::loxP-hphMX-loxP IV1510386::kanMX-can1-100*	W303-1A

		RNH2kanF and RNH2kanR		
SJR3625-9B	*rnh1*Δ *rnh201*Δ	SJR3615-4 transformed with PCR fragment amplified from pSR879 using primers RNH1kanF and RNH1kanR	*MAT***a** *leu2-3,112 his3-11,15 trp1-1 ura3-1 ade2-1 RAD5 rnh1Δ::loxP-natMX-loxP rnh201Δ::loxP-hphMX-loxP IV1510386::kanMX-can1-100*	W303-1A
SJR3616-3	*rnh201*Δ	SJR3586 transformed with PCR fragment amplified from pSR955 using primers RNH2kanF and RNH2kanR.	*MATα ura3 gal2 ho::hisG ade2-1 can1Δ::natMX rnh201Δ::loxP-hphMX-loxP IV1510386::SUP4-o*	YJM789
SJR3626-3	*rnh1*Δ *rnh201*Δ	SJR3616-3 transformed with PCR fragment amplified from pUG6 using RNH1kanF and RNH1kanR	*MATα ura3 gal2 ho::hisG ade2-1 can1Δ::natMX rnh201Δ::loxP-hph-loxP rnh1Δ::loxP-kanMX-loxP IV1510386::SUP4-o*	YJM789
YJM799	Wild type	John McCusker	*MATα ura3 gal2 ho::hisG*	YJM789
YJM790	Wild type	John McCusker	*MAT***a** *ho::hisG lys2 gal2*	YJM789
KOK3	Wild type	W1588-4c transformed with PCR fragment amplified from pUG6 using primers Forward Sequence and Reverse Sequence.	*MAT***a** *can1-100 trp1-1 ade2-1 his3-11,15 leu2-3,112 ura3Δ::loxP-kanMX-loxP*	W303-1A
KO5	*rnh1*Δ *rnh201*Δ	SJR3625-9B x SJR3626-3	*MAT***a***/MATα ho::hisG/ho::hisG ade2-1/ade2-1 ura3-1/ura3 GAL2/gal2 trp1-1/TRP1 his3-11,15/HIS3 leu2-3,112/LEU2 can1-100/CAN1 rnh201Δ::loxP-hphMX-loxP/rnh201Δ::loxP-hphMX-loxP rnh1Δ::loxP-natMX-loxP/rnh1Δ::loxP-kanMX-loxP IV1510386::kanMX-can1-100/IV1510386::SUP4-o*	W303-1A/YJM789
KO30	Wild type	SJR3626-3 x YJM790	*MAT***a***/MATα ho::hisG/ho::hisG gal2/gal2 ade2-1/ADE2 URA3/ura3 lys2/LYS2 CAN1/can1Δ::natMX RNH201/rnh201Δ::loxP-hphMX-loxP RNH1/rnh1Δ::loxP-kanMX-loxP IV1510386/IV1510386::SUP4-o*	YJM789
KO32	*rnh1*Δ *rnh201*Δ	Spore from KO30	*MAT***a** *can1Δ::natMX ade2-1 ura3 ho::hisG gal2 rnh1::loxP-kanMX-loxP rnh201::loxP-hphMX-loxP*	YJM789
KO35	Wild type	JSC19-1 transformed with PCR fragment amplified from S288c using primers IVURA3F and IVURA3R.	*MATα ade2-1 ura3 gal2 ho::hisG can1Δ::nat IV1510386::URA3*	YJM789

KO36	Wild type	Cre-expressing plasmid pSH47 used to excise the kanMX marker in KOK3	*MAT**a** can1-100 trp1-1 ade2-1 his3-11,15 leu2-3,112 ura3Δ::loxP*	W303-1A
KO49	Wild type	KO32 x KO35	*MAT**a**/MATα ade2-1/ade2-1 ura3/ura3 gal2/gal2 ho::hisG/ho::hisG can1Δ::nat/can1Δ::nat rnh1Δ ::loxP-kanMX-loxP/RNH1 rnh201Δ::loxP-hphMX-loxP/RNH201 IV1510386/IV1510386::URA3*	YJM789/ YJM789
KO52	Wild type	SJR3625-9B x W303-1B	*MAT**a**/MATα leu2-3,112/leu2-3,112 his3-11,15/his3-11,15 trp1-1/trp1-1 ura3-1/ura3-1 ade2-1/ade2-1 CAN1/can1-100 IV1510386::kanMX-can1-100/IV1510386 rnh1Δ::loxP-natMX-loxP/RNH1 rnh201Δ::loxP-hphMX-loxP/RNH201*	W303-1A/ W303-1A
KO57	*rnh1*Δ	Spore of KO49	*MATα ade2-1 ura3 gal2 ho::hisG can1Δ::nat IV1510386::URA3 rnh1Δ::loxP-kanMX-loxP*	YJM789
KO63	*rnh1*Δ *rnh201*Δ	Spore from KO52	*MATα leu2-3,112 his3-11,15 trp1-1 ura3-1 ade2-1 can1-100 rnh1Δ::loxP-natMX-loxP rnh201Δ::loxP-hphMX-loxP*	W303-1A
KO70	*rnh1*Δ	Spore of KO52	*MAT**a** leu2-3,112 his3-11,15 trp1-1 ura3-1 ade2-1 can1-100 rnh1Δ::loxP-nat-loxP*	W303-1A
KO73	*rnh1*Δ	KO70 x KO57	*MAT**a**/MATα HO/ho::hisG ade2-1/ade2-1 ura3-1/ura3 GAL2/gal2 trp1-1/TRP1 his3-11,15/HIS3 leu2-3,112/LEU2 can1-100/CAN1 rnh1Δ::loxP-natMX-loxP/rnh1Δ::loxP-kanMX-loxP IV1510386::URA3/IV1510386*	W303-1A/ YJM789
KO75	*rnh201*Δ	SJR3616-3 x SJR3615-4	*MAT**a**/MATα HO/ho::hisG ade2-1/ade2-1 ura3-1/ura3 GAL2/gal2 trp1-1/TRP1 his3-11,15/HIS3 leu2-3,112/LEU2 can1-100/CAN1 rnh201Δ::loxP-hphMX-loxP/rnh201Δ::loxP-hphMX-loxP IV1510386::URA3/IV1510386*	W303-1A/ YJM789
KO119	Wild type	YJM799 transformed with transformed with PCR fragment amplified from SMY710 using primers ADE2_XV_F and ADE2_XV_R	*MATα ura3 gal2 ho::hisG ade2Δ::kanMX*	YJM789
KO124	Wild type	KO119 transformed with transformed with PCR fragment amplified from	*MATα ade2Δ::kanMX ura3 ho::hisG gal2 IV1495420::ADE2*	YJM789

		S288c using primers IVADE2_3_F and IVADE2_3_R		
KO125	Wild type	KO124 x KO32	*MAT**a**/MATα can1Δ::natMX/CAN1 ade2-1/ade2Δ::kanMX ura3/ura3 ho::hisG/ho::hisG gal2/gal2 rnh1Δ::loxP-kanMX-loxP/RNH1 rnh201Δ::loxP-hphMX-loxP/RNH201 IV1495420/IV1495420::ADE2*	YJM789/ YJM789
KO127	*rnh1*Δ *rnh201*Δ	Spore from KO125	*MATα ade2-1 ura3 ho::hisG gal2 can1Δ::natMX rnh1Δ::loxP-kanMX-loxP rnh201Δ::loxP-hphMX-loxP IV1495420::ADE2*	YJM789
KO128	*rnh1*Δ	Spore from KO125	*MATα ade2-1 ura3 ho::hisG gal2 can1Δ::natMX rnh1Δ::loxP-kanMX-loxP IV1495420::ADE2*	YJM789
KO131	*rnh201*Δ	Spore from KO125	*MATα ade2-1 ura3 ho::hisG gal2 rnh201Δ::loxP-hphMX-loxP IV1495420::ADE2*	YJM789
KO132	*rnh1*Δ *rnh201*Δ	KO127 x SJR3625-9B	*MAT**a**/MATα leu2-3,112/LEU2 his3-11,15/HIS3 trp1-1/TRP1 ura3-1/ura3 ade2-1/ade2-1 rnh1Δ::loxP-natMX-loxP /rnh1Δ::loxP-kanMX-loxP rnh201Δ::loxP-hphMX-loxP/rnh201Δ::loxP-hphMX-loxP ho::hisG/ho::hisG GAL2/gal2 IV1510386::kanMX-can1-100/IV1510386 IV1495420/IV1495420::ADE2*	W303-1A/ YJM789
KO135	*rnh201*Δ	KO130 x SJR3615-4	*MAT**a**/MATα leu2-3,112/LEU2 his3-11,15/HIS3 trp1-1/TRP1 ura3-1/ura3 HO/ho::hisG ade2-1/ade2-1 GAL2/gal2 CAN1/can1Δ::natMX IV1510386::kanMX-can1-100/IV1510386 rnh201Δ::loxP-hphMX-loxP/rnh201Δ::loxP-hphMX-loxP IV1495420/IV1495420::ADE2*	W303-1A/ YJM789
KO171	Wild type	KOK3 transformed with transformed with PCR fragment amplified from pUG72 using primers KL_URA3_F and KL_URA3_R.	*MAT**a** can1-100 trp1-1 ade2-1 his3-11,15 leu2-3,112 ura3Δ::loxP-kanMX-loxP IV1495420::loxP-URA3Kl-loxP*	W303-1A
KO172	Wild type	KO171 x KO63	*MAT**a**/MATα can1-100/can1-100 trp1-1/trp1-1 ade2-1/ade2-1 leu2-3,112/leu2-3,112 his3-11,15/his3-11,15 ura3Δ::loxP-kanMX-loxP/ura3-1 RNH201/rnh201Δ::loxP-hphMX-loxP RNH1/rnh1Δ::loxP-natMX-loxP IV1495420::loxP-URA3Kl-loxP/IV1495420*	W303-1A/ W303-1A

KO175	*rnh1*Δ *rnh201*Δ	Spore from KO172	*MAT***a** *can1-100 trp1-1 ade2-1 ura3-1 leu2-3,112 his3-11,15 rnh201Δ::loxP-hph-loxP rnh1Δ::loxP-natMX-loxP IV1495420::loxP-URA3KI-loxP*	W303-1A
KO176	*rnh1*Δ *rnh201*Δ	Spore from KO172	*MATα can1-100 trp1-1 ade2-1 leu2-3,112 his3-11,15 ura3-1 rnh201Δ::loxP-hphMX-loxP rnh1Δ::loxP-natMX-loxP IV1495420::loxP-URA3KI-loxP*	W303-1A
KO179	*rnh201*Δ	Spore from KO172	*MAT***a** *can1-100 trp1-1 ade2-1 ura3-1 leu2-3,112 his3-11,15 rnh201Δ::loxP-hph-loxP IV1495420::loxP-URA3KI-loxP*	W303-1A
KO185	*rnh1*Δ	Spore from KO172	*MAT***a** *can1-100 trp1-1 ade2-1 ura3-1 leu2-3,112 his3-11,15 rnh1Δ::loxP-natMX-loxP IV1495420::loxP-URA3KI-loxP*	W303-1A
KO187	*rnh1*Δ	KO185 x KO128	*MAT***a***/MATα HO/ho::hisG ade2-1/ade2-1 ura3-1/ura3 GAL2/gal2 trp1-1/TRP1 his3-11,15/HIS3 leu2-3,112/LEU2 can1-100/can1Δ::natMX rnh1Δ::loxP-natMX-loxP/rnh1Δ::loxP-kanMX-loxP IV1495420::loxP-URA3KI-loxP/IV1495420::ADE2*	W303-1A/ YJM789
KO188	*rnh201*Δ	KO179 x KO131	*MAT***a***/MATα HO/ho::hisG ade2-1/ade2-1 ura3-1/ura3 GAL2/gal2 trp1-1/TRP1 his3-11,15/HIS3 leu2-3,112/LEU2 can1-100/can1Δ::natMX rnh201Δ::loxP-natMX-loxP/rnh201Δ::loxP-kanMX-loxP IV1495420::loxP-URA3KI-loxP/IV1495420::ADE2*	W303-1A/ YJM789
KO189	*rnh1*Δ *rnh201*Δ	KO175 x KO127	*MAT***a***/MATα HO/ho::hisG ade2-1/ade2-1 ura3-1/ura3 GAL2/gal2 trp1-1/TRP1 his3-11,15/HIS3 leu2-3,112/LEU2 can1-100/CAN1 rnh201Δ::loxP-hphMX-loxP/rnh201Δ::loxP-hphMX-loxP rnh1Δ::loxP-natMX-loxP/rnh1Δ::loxP-kanMX-loxP IV1495420::loxP-URA3KI-loxP/IV1495420::ADE2*	W303-1A/ YJM789
KO198	Wild type	KO171 x KO124	*MAT***a***/MATα HO/ho::hisG ade2-1/ade2Δ::kanMX ura3Δ ::loxP-kanMX-loxP/ura3 GAL2/gal2 trp1-1/TRP1 his3-11,15/HIS3 leu2-3,112/LEU2 can1-100/CAN1 IV1495420::loxP-URA3KI-loxP/IV1495420::ADE2*	W303-1A/ YJM789
KO200	*pol2-M644L*	*pol2-M644L* introduced into KO36 by two-step allele replacement using AgeI-digested p173-pol2-M644L	*MAT***a** *can1-100 trp1-1 ade2-1 his3-11,15 leu2-3,112 ura3Δ::loxP pol2-M644L*	W303-1A
KO201	Wild type	KO200 x KO176	*MAT***a***/MATα can1-100/can1-100 trp1-1/trp1-1 ade2-1/ade2-1 his3-11,15/his3-11,15 leu2-3,112/leu2-3,112*	W303-1A/ W303-1A

			ura3Δ::loxP/ura3-1 pol2-M644L/POL2 RNH1/rnh1Δ::loxP-natMX-loxP rnh201Δ::loxP-hphMX-loxP/RNH201 IV1495420/IV1495420::ADE2	
KO204	*rnh201*Δ *pol2-M644L*	Spore from KO201	*MAT***a** *can1-100 trp1-1 ade2-1 his3-11,15 leu2-3,112 ura3-1 pol2-M644L rnh201Δ::loxP-hphMX-loxP IV1495420::loxP-URA3K.L-loxP*	W303-1A
KO207	*rnh201*Δ *pol2-M644L*	*pol2-M644L* introduced into KO131 by two-step allele replacement using *Age*I-digested p173-pol2-M644L	*MATα ade2-1 can1Δ::natMX ura3 ho::hisG gal2 pol2-M644L rnh201Δ::loxP-hphMX-loxP IV1495420::ADE2*	YJM789
KO213	*pol2-M644L*	KO124 after two-step transplacement using *Age*I-digested p173-pol2-M644L	*MATα ade2Δ::kanMX ura3 ho::hisG gal2 IV1495420::ADE2 pol2-M644L*	YJM789
KO214	Wild type	KO207 x KO32	*MAT***a***/MATα can1Δ::natMX/CAN1 ade2-1/ade2-1 ura3/ura3 ho::hisG/ho::hisG gal2/gal2 rnh1Δ::loxP-kanMX-loxP/RNH1 rnh201Δ::loxP-hphMX-loxP/RNH201 POL2/pol2M644L IV1495420/IV1495420::ADE2*	YJM789/ YJM789
KO218	*rnh201*Δ *pol2-M644L*	Spore from KO214	*MATα ade2-1 ura3 gal2 ho::hisG pol2-M644L can1::ΔnatMX rnh201Δ::loxP-hphMX-loxP IV1495420::ADE2*	YJM789
KO234	*pol2-M644L/ pol2-M644L*	KO213 x KO200	*MAT***a***/MATα HO/ho::hisG ade2-1/ade2-1 ura3-1/ura3 GAL2/gal2 trp1-1/TRP1 his3-11,15/HIS3 leu2-3,112/LEU2 can1-100/CAN1 pol2-M644L/pol2-M644L IV1495420::loxP-URA3KI-loxP/IV1495420::ADE2*	W303-1A/ YJM789
KO244	*rnh201*Δ *pol2-M644L*	KO218 x KO204	*MAT***a***/MATα HO/ho::hisG ade2-1/ade2-1 ura3-1/ura3 GAL2/gal2 trp1-1/TRP1 his3-11,15/HIS3 leu2-3,112/LEU2 can1-100/can1Δ::natMX rnh201Δ::loxP-hphMX-loxP/rnh201Δ::loxP-hphMX-loxP pol2-M644L/pol2-M644L IV1495420::loxP-URA3KI-loxP/IV1495420::ADE2*	W303-1A/ YJM789

Table S2. Plasmid list

Plasmid	Relevant feature	Source	Strains constructed
pFA6-kanMXpGAL(x3HA)	*kanMX-pGAL* cassette	Longtine *et al.* 1998	PG309(2)
p173-pol2-M644L	*pol2-M644L* allele	Nick McElhinny *et al.* 2010	KO200, KO207, KO213
pAG25	*natMX*	Goldstein and McCusker 1999	PG308
pSH47	*pGAL1-Cre*	Gueldener *et al.* 2002	KO36
pUG72	*loxP-URA3Kl-loxP*	Gueldener *et al.* 2002	KO171
pSR879	*loxP-natMX-loxP*	Kim *et al.* 2013	SJR3625-9B
pSR955	*loxP-hphMX-loxP*	Kim *et al.* 2013	SJR3615-4, SJR3616-3
pUG6	*loxP-kanMX-loxP*	Gueldener *et al.* 2002	SJR3626-3, KOK3

Table S3. Primers list

Primer	Sequence (5′ to 3′)	Strains constructed (purpose)
RNH1KANF	ATGGCAAGGCAAGGGAACTTCTACGCGGTTAGAAAGGGCAGGGAAA CTGGGATCTATAATCAGCTGAAGCTTCGTACG	SJR2626-3, SJR3625-9B (construct *RNH1* deletion)
RNH1KANR	GCATTATCGTCTAGATGCTCCTTTCTTCGCCAGAAAATCTGCCATTTC ATTTCCTGGATCAGGCCACTAGTGGATCTG	SJR2626-3, SJR3625-9B (construct *RNH1* deletion)
RNH1UPF	TGGCAGCACAATAATACACG	KO127, KO128, SJR3626-3, SJR3625-9b (confirm *rnh1*Δ)
RNH1DWNR	CACGCTTATAGATAGTTATCG	KO127, KO128, SJR3626-3, SJR3625-9b (confirm *rnh1*Δ)
RNH2KANF	CTAATGAGAGTGTCGAAAAACCTTGAAAACAACTACTGCACACCAAAT TGATACGATTAACAGCTGAAGCTTCGTACG	SJR3615-4, SJR3616-3 (*RNH201* deletion)
RNH2KANR	GCTTCACGGATAGTAGAAACGGCAAAGCATAGTAGCAGATGACTTGT ATGAGTTATTGAAAGGCCACTAGTGGATCTG	SJR3615-4, SJR3616-3 (*RNH201* deletion)
RNH2UPF	TTGCGACGCCTGCCAATGC	SJR3615-4, SJR3616-3 (confirm *rnh201*Δ)
RNH2DWR	TCGTTCCGGTTGGTTGTCTC	SJR3615-4, SJR3616-3 (confirm *rnh201*Δ)
KL_URA3_F	CGGGTAGAATCAATGCAATCAGTGGTAATTATCTAGATGACGTCCTTT ATGACCTTGACACCCCTGCAGCTGAAGCTTCGTACG	KO171 (insertion of *URA3KI* at end of chr. IV)
KL_URA3_R	TGTGGTGACAACCTAACCCTTTCGTTGATACTAGTTTGAAGGTTATCA ATATCCTGAATTAGAGTTGTGGAGGCCACTAGTGGATCTG	KO171 (insertion of *URA3KI* at end of chr. IV)
IVADE2_3_F	CGGGTAGAATCAATGCAATCAGTGGTAATTATCTAGATGACGTCCTTT ATGACCTTGACACCCCTGGTTGAGAAGCCGAGAATTTTGTA	KO124 (insertion of *ADE2* at end of chr. IV)
IVADE2_3_R	TGTGGTGACAACCTAACCCTTTCGTTGATACTAGTTTGAAGGTTATCA ATATCCTGAATTAGAGTTGTGGTCCTCGGTTCTGCATTGAG	KO124 (insertion of *ADE2* at end of chr. IV)
IVURA3F	GCTTTACAGGACCTATTTTTCATACGTTATGCACTTCATTCTTTTTGTC GGTTTGATACCAGCAGAATCTAACGCTAGAGCAGACGCTCAT	KO35 (insertion of *URA3* at end of chr. IV)
IVURA3R	AAGCGCTGCTGCGTTTTCGAGGTATGGCTTCTGCCGGGCTAACGTTC AAATTAAAGGAACAGATTCCCGGGTAATAACTGA	KO35 (insertion of *URA3* at end of chr. IV)
EXT1510386F	CATTGGAGCGAATGATGACG	KO35 (confirmation of *URA3* insertion on chr. IV)
EXT1510386R	TGTGCAATCGTTGTCAAGTTGG	KO35 (confirmation of *URA3* insertion on chr. IV)
Forward Sequence	TGCCCAGTATTCTTAACCCAACTGCACAGAACAAAAACCTGCAGGAA ACGAAGATAAATCCAGCTGAAGCTTCGTACG	KOK3 (deletion of *URA3* locus)
Reverse	TTAAATTGAAGCTCTAATTTGTGAGTTTAGTATACATGCATTTACTTAT	KOK3 (deletion of *URA3* locus)

Sequence	AATACAGTTTTAGGCCACTAGTGGATCTG	
ADE2_XV_R	GGTGCGTAAAATCGTTGGAT	KO119, KO127, KO128 (to insert *ade2Δ::kanMX* in KO119 and to determine whether KO127 and KO128 had *ade2-1* or *ade2Δ::kanMX*)
ADE2_XV_F	ATCCTCGGTTCTGCATTGAG	KO119, KO127, KO128 (to insert *ade2Δ::kanMX* in KO119 and to determine whether KO127 and KO128 had *ade2-1* or *ade2Δ::kanMX*)
Pol2DigestF1	GAAAAGCCACAGCACCTTTC	KO200, KO207, spores of KO214 and KO201 (confirmation of *pol2-M644L)*
Pol2DigestR1	TTGGACAGATTTCCCTTCCA	KO200, KO207, spores of KO214 and KO201 (confirmation of *pol2-M644L)*
MATaF	ACTCCACTTCAAGTAAGAGTTTG	Many strains (diagnosis of mating type)
MATalphaF	GCACGGAATATGGGACTACTTCG	Many strains (diagnosis of mating type)
MATR	AGTCACATCAAGATCGTTTATGG	Many strains (diagnosis of mating type)
extF3	AATGCGGGTAGAATCAATGC	KO124, KO171 (confirmation of *ADE2* or *URA3KI* insertion on chr. IV)
extR3	AGGTGATGGGAAATCGAGTG	KO124, KO171 (confirmation of *ADE2* or *URA3KI* insertion on chr. IV)
KANF222	AATTTATGCCTCTTCCGACC	KOK3 (confirmation of *URA3* deletion)
URAR1128	GAAATCATTACGACCG	KOK3 (confirmation of *URA3* deletion)
Tel1NATF	ATTCGAAAAAAAAGCCTTCAAAGAAAAGGGAAATCAGTGTAACATAGACGCGTACGCTGCAGGTCGAC	PG308 (replacement of *tel1::kanMX* with *tel1::natMX*)
Tel1NATR	TTCGTATTTCTATAAACAAAAAAAAGAAGTATAAAGCATCTGCATAGCAAATCGATGAATTCGAGCTCG	PG308 (replacement of *tel1::kanMX* with *tel1::natMX*)
MRC1pgalF	GGAAGTTCGTTATTCGCTTTTGAACTTATCACCAAATATTGAATTCGAGCTCGTTTAAAC	PG309(2) (to insert the *GAL1* promoter and *kanMX* upstream of *MRC1*)
MRC1pgalR	TTGCAGTCAACGAGGACAAAGCATGCAAGGCATCATCCATGCACTGAGCAGCGTAATCTG	PG309(2) (to insert the *GAL1* promoter and *kanMX* upstream of *MRC1*)

Table S4. Strains used in different assays of LOH

Genotype	Sub-culturing	Sectoring assay	RCO mapping in sectored colonies	Rate of 5FOA resistance
wild-type	KO198	KO198	KO198	KO198
*rnh1*Δ	KO73	KO187	KO187	KO187
pol2-M644L	KO234	KO234	KO234	KO234
*rnh201*Δ	KO75	KO188	KO188 and KO135	KO188
*rnh201*Δ *pol2-M644L*	KO244	KO244	KO244	KO244
*rnh1*Δ *rnh201*Δ	KO5	KO189	KO132	KO189

Tables S5-S8

Available for download as Excel files at
www.genetics.org/lookup/suppl/doi:10.1534/genetics.115.182725/-/DC1

Table S5 LOH events in sub-cultured strains

Table S6 Deletions-Duplications, sub-cultured strains

Table S7 Trisomy

Table S8 LOH events on chromosome IV in sectored colonies

Table S9. References used to determine locations of genomic elements.[1]

Genomic elements	Data source
Ty element	SGD; YeastMine
Solo LTR	SGD; YeastMine
Centromeres	SGD; YeastMine
Intron-containing genes	SGD; YeastMine
ARS elements	SGD; YeastMine
tRNA genes	SGD; YeastMine
Long genes	SGD; YeastMine
Regions of high transcription	SGD; YeastMine
Regions of low transcription	SGD; YeastMine
ORFs with high GC content	SGD; YeastMine
High G content on the non-transcribed strand	SGD; YeastMine
Sites of Rbp3 accumulation in S phase	Fachinetti *et al*. 2010
TER sites	Fachinetti *et al*. 2010
TER sites related to high transcription	Fachinetti *et al*. 2010
Sites of Rrm3 accumulation	Azvolinsky *et al.* 2009
Palindromic sequences	Lisnic *et al.* 2005
Sites of G4 quadruplex formation (predicted by sequence context *in silico*)	Capra *et al.* 2010
Sites of differential transcription in response to NMM[2]	Hershman *et al.* 2008
Regions of transcription-transcription conflicts resolved by Elc1p[3]	Hobson *et al*. 2012
Tracts of poly A or poly T $\geq$ 25 bp	SGD
Sites of RNA/DNA hybrid accumulation in *rnh1 rnh201*	Chan *et al.* 2014

[1]Most of the genomic elements were identified in Saccharomyces Genome Database (SGD) using the YeastMine tool (described: http://www.yeastgenome.org/help/video-tutorials/yeastmine). The criteria used to determine the number each elements in the genome are described in File S1. We chose to identify tracts of poly A or poly T > 25 bp based on a personal communication from Doug Koshland (University of California, Berkeley) who found an association between such tracts and the locations of R-loops.
[2]NMM is an abbreviation for N-methyl mesoporphyrin IX, a drug that binds G4 quadruplex structures.
[3]Elc1p is a protein required to remove stalled RNA polymerase II complexes (Hobson *et al*., 2012).

Table S10. Number of genomic elements represented on the microarrays

Element	# elements per genome	# elements on whole-genome array[1]	# elements in *rnh201Δ*[2]	# elements in *rnh201Δ pol2-M644L*[2]	# elements in *rnh1Δ rnh201Δ*[2]	# elements on chromosome IV array[3]
Ty elements	50	48	48	48	35	8
Solo LTRs	291	280	280	276	246	19
Centromeres	16	16	16	16	16	1
Intron-containing genes	345	331	331	323	287	24
ARS elements	352	317	317	308	275	28
tRNA genes	275	274	274	270	236	23
Long genes	306	306	306	295	259	28
Regions of high transcription	330	329	329	318	270	36
Regions of low transcription	328	312	312	303	272	20
ORFs with high GC content	115	115	115	114	96	8
High G content on the non-transcribed strand	41	41	41	40	34	1
Sites of Rbp3 accumulation in S phase	93	93	93	93	70	11
TER sites	71	71	71	69	69	3
TER sites related to high transcription	58	58	58	56	56	3
Sites of Rrm3 accumulation	115	112	112	112	103	6
Palindromic sequences	611	589	589	573	517	51
Sites of G4 quadruplex formation (predicted by sequence context *in silico*)	636	543	543	536	480	20
Sites of differential transcription in response to NMM	114	107	107	105	96	7
Regions of transcription-transcription conflicts resolved by Elc1.	144	144	144	137	125	13

Tracts of poly A or poly T ≥ 25 bp	43	41	41	40	36	3
Sites of RNA/DNA hybrid accumulation in *rnh1 rnh201*	163	129	129	127	112	10

[1]In our analysis, we examined twenty-one types of genomic elements. The references for the locations of these elements are described in Table S9 and in File S1. The total size of the yeast genome, as presented in SGD, is about 12.1 Mb. Since this calculated size counts only two of the approximately 150 ribosomal rRNA genes, there are about 12.1 Mb of single-copy yeast sequences. Our whole-genome microarrays omit most repetitive sub-telomeric repeats. 11.6 Mb of the genome are represented on our whole-genome arrays (details in Dataset S1 of Song *et al*., 2014). The coordinates and sequences of all oligonucleotides on the whole-genome arrays are in Table S5 of St. Charles *et al.* (2012).

[2]In several of the mutant strains, LOH events existed in the starting strains. These regions were omitted from the analysis. The summary of these omissions is: 1) *rnh201*Δ (no pre-existing LOH events, therefore, no omissions necessary), 2) *rnh201*Δ *pol2-M644L* (sequences distal to SGD coordinate 592645 on chromosome XIII were homozygous and deleted from the analysis; 11.3 Mb were in the remaining analysis), and 3) *rnh1 rnh201* (most of these strains had terminal LOH events beginning at SGD coordinate 1263027 on chromosome IV, and coordinate 447834 on chromosome XII; the remaining portion of the genome was about 11.0 Mb). The numbers of elements in each strain were corrected for these deletions.

[3]The chromosome IV-specific microarrays monitor SNPs from *CEN4* to near the right telomere of chromosome IV (coordinate 1511708), a region of about 1.1 Mb). The locations of SNPs on the chromosome IV-specific arrays are in Table S9 of St. Charles and Petes (2013).

Table S11. Association of LOH events in sub-cultured strains with various genomic elements.

Genome Feature	*rnh201Δ*			*rnh201Δ pol2-M644L*			*rnh1Δ rnh201Δ*		
	Exp inside: outside	Obs inside: outside	p-value	Exp inside: outside	Obs inside: outside	p-value	Exp inside: outside	Obs inside: outside	p-value
Ty elements	8:904	7:905	0.863	5:811	6:810	0.823	9:761	5:765	0.240
Solo LTRs	33:5287	24:5296	0.138	22:4670	12:4680	0.042	51:5779	66:5764	0.041
Centromeres	2:302	0:304	0.286	1:271	3:269	0.133	3:349	3:349	1.000
Intron- containing genes	39:6250	30:6259	0.173	26:5465	22:5469	0.493	60:6738	59:6739	1.000
ARS elements	37:5986	31:5992	0.362	25:5211	19:5217	0.269	57:6367	54:6370	0.729
tRNA genes	32:5174	22:5184	0.092	22:4568	16:4574	0.238	50:5626	48:5628	0.823
Long genes	46:5768	45:5769	0.920	31:4984	35:4980	0.527	72:6220	67:6225	0.597
Genes with high transcription	39:6212	35:6216	0.578	25:5381	25:5381	1.000	58:6564	63:6559	0.554
Genes with low transcription	37:5891	37:5891	1.000	24:5127	27:5124	0.610	57:6367	51:6373	0.467
ORFs with high GC content	14:2171	9:2176	0.227	9:1929	15:1923	0.066	20:2246	14:2252	0.218
High G content on the non-transcribed strand	5:774	4:775	0.823	3:677	1:679	0.387	7:763	9:761	0.572
Sites of Rbp3 accumulation in S phase	11:1756	11:1756	1.000	7:1574	6:1575	0.842	16:1766	20:1762	0.377
TER sites	8:1341	5:1344	0.377	6:1167	8:1165	0.538	18:1500	15:1503	0.554
TER sites related to high transcription	9:1093	5:1097	0.242	6:946	5:947	0.842	14:1218	11:1221	0.498
Sites of Rrm3 accumulation in S phase	13:2115	17:2111	0.330	9:1895	12:1892	0.406	21:2311	12:2320	0.063
Palindromic sequences	70:11121	80:11111	0.254	46:9695	42:9699	0.603	110:12320	85:12345	0.008
Sites of G4 quadruplex formation (predicted *in silico*)	64:10253	45:10272	0.020	43:9069	47:9065	0.597	99:11121	73:11147	0.010
Regions of differential transcription in response to NMM	13:2020	12:2021	0.888	8:1777	5:1780	0.377	20:2246	15:2251	0.313
Regions of transcription-transcription conflicts resolved by Elc1	17:2719	18:2718	0.920	11:2318	18:2311	0.050	27:2987	25:2989	0.777
Regions of RNA/DNA hybrid accumulation in the *rnh1 rnh201* mutant	15:2436	14:2437	0.888	10:2149	13:2146	0.427	24:2660	28:2656	0.475
Poly A or poly T tracts $\geq$ 25 bp	5:774	8:771	0.262	3:677	2:678	0.777	8:850	6:852	0.597

The details of the association analysis are described in File S1. In brief, we summed the amount of sequences inside the LOH association windows and the amount of sequences located outside of those windows for all isolates of the individual mutant strains. Based on the total number of elements examined by the array (Table S10), we calculated the number of elements expected within and outside of those windows; this information is summarized in the column labeled “Exp inside:outside.” We then counted the elements within and outside of the association windows (Column “Obs inside:outside”). The observed and expected values were compared using Chi-square “Goodness of Fit” test. Because of the multiple comparisons, we then applied the Benjamini-Hochberg correction to the data (Benjamini and Hochberg, 1995). Following this correction, none of the LOH events in any of the strains were significantly associated with any of the tested genomic elements.

Table S12. Association of LOH events in sectored colonies with various genomic elements on the right arm of chromosome IV

	*rnh201*Δ			*rnh1*Δ *rnh201*Δ		
Genome Feature	**expected inside: outside**	**observed inside: outside**	**p-value**	**expected inside: outside**	**observed inside: outside**	**p-value**
Ty elements	3:165	2:166	0.777	3:109	4:108	0.777
Solo LTRs	5:394	3:396	0.498	7:259	10:256	0.340
Centromeres	0:21	0:21	1.000	0:14	0:14	1.000
Intron-containing genes	7:497	8:496	0.841	8:328	12:324	0.210
ARS elements	8:580	9:579	0.862	10:382	7:385	0.420
tRNA genes	6:477	5:478	0.585	8:314	9:313	0.862
Long genes	10:578	15:573	0.150	11:381	13:379	0.647
Genes with high transcription	10:746	8:748	0.632	13:491	17:487	0.327
Genes with low transcription	6:414	4:416	0.532	7:273	4:276	0.340
ORFs with high GC content	2:166	1:167	0.718	3:109	1:111	0.380
Regions with high G content on the non-transcribed strand	0:21	0:21	1.000	0:14	1:13	1.000
Sites of Rbp3 accumulation in S phase	3:228	3:228	1.000	4:150	3:151	0.806
TER sites	1:62	1:62	1.000	1:41	1:41	1.000
TER sites related to high transcription	1:62	1:62	1.000	1:62	1:62	1:62
Sites of Rrm3 accumulation in S phase	2:124	1:125	0.718	2:82	1:83	0.718
Palindromic sequences	14:1057	17:1054	0.498	18:696	27:687	0.043
Sites of G4 quadruplex formation	6:414	6:414	1.000	7:273	9:271	0.566
Regions of differential transcription in response to NMM	2:145	1:146	0.718	2:96	2:96	1.000
Regions of t ranscription-transcription conflicts resolved by Elc1	4:269	4:269	1.000	5:177	8:174	0.256
Sites of RNA/DNA hybrid accumulation in the *rnh1 rnh201* mutant	3:207	4:206	0.777	4:136	7:133	0.206
Poly A or poly T tracts $\geq$ 25bp	1:62	1:62	1.000	1:41	2:40	0.610

The associations were examined by the same methods described in Table S11, except analysis was limited to the right arm of chromosome IV. None of the associations was statistically significant after applying the correction for testing multiple samples.

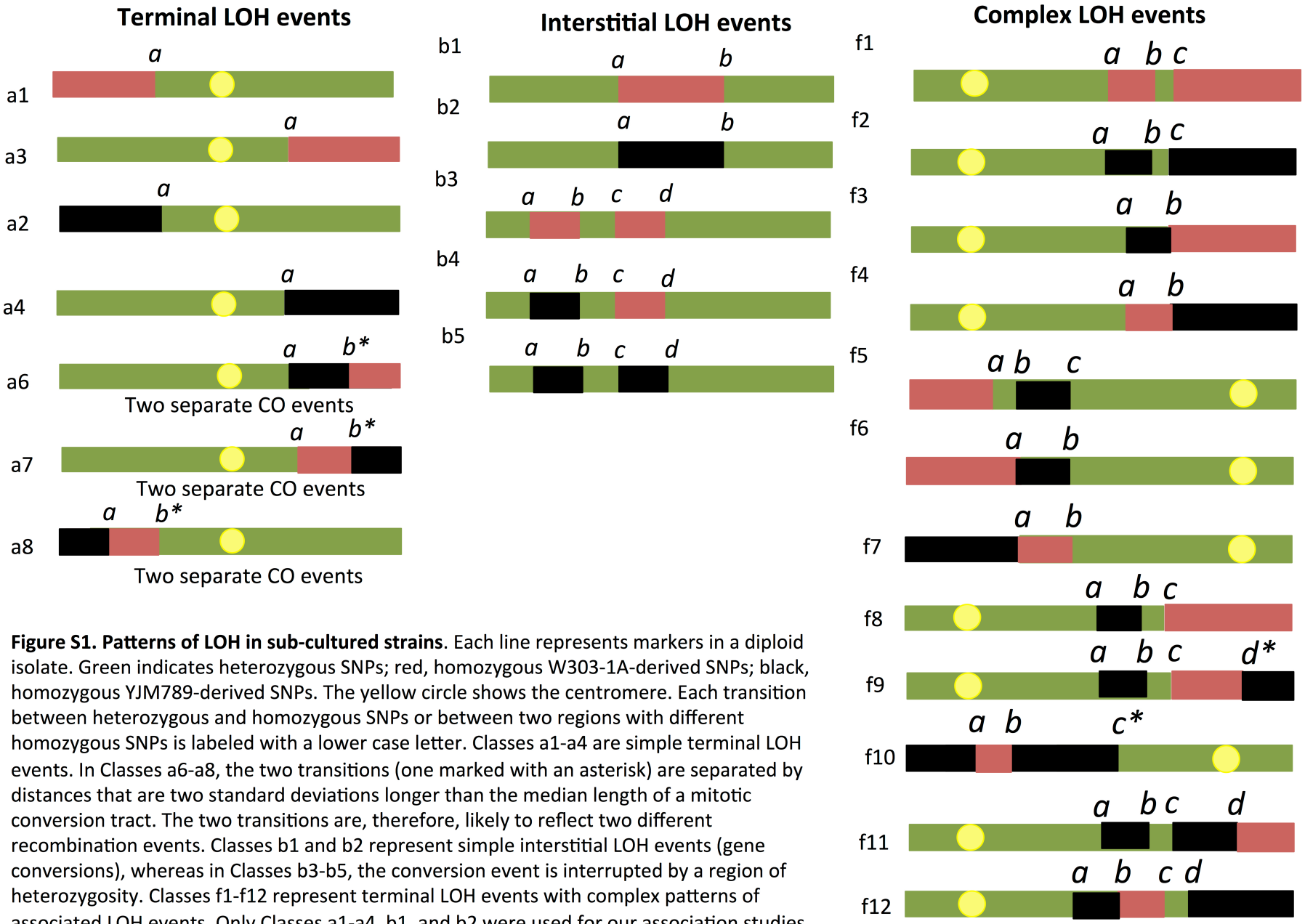

Figure S1. Patterns of LOH in sub-cultured strains. Each line represents markers in a diploid isolate. Green indicates heterozygous SNPs; red, homozygous W303-1A-derived SNPs; black, homozygous YJM789-derived SNPs. The yellow circle shows the centromere. Each transition between heterozygous and homozygous SNPs or between two regions with different homozygous SNPs is labeled with a lower case letter. Classes a1-a4 are simple terminal LOH events. In Classes a6-a8, the two transitions (one marked with an asterisk) are separated by distances that are two standard deviations longer than the median length of a mitotic conversion tract. The two transitions are, therefore, likely to reflect two different recombination events. Classes b1 and b2 represent simple interstitial LOH events (gene conversions), whereas in Classes b3-b5, the conversion event is interrupted by a region of heterozygosity. Classes f1-f12 represent terminal LOH events with complex patterns of associated LOH events. Only Classes a1-a4, b1, and b2 were used for our association studies.

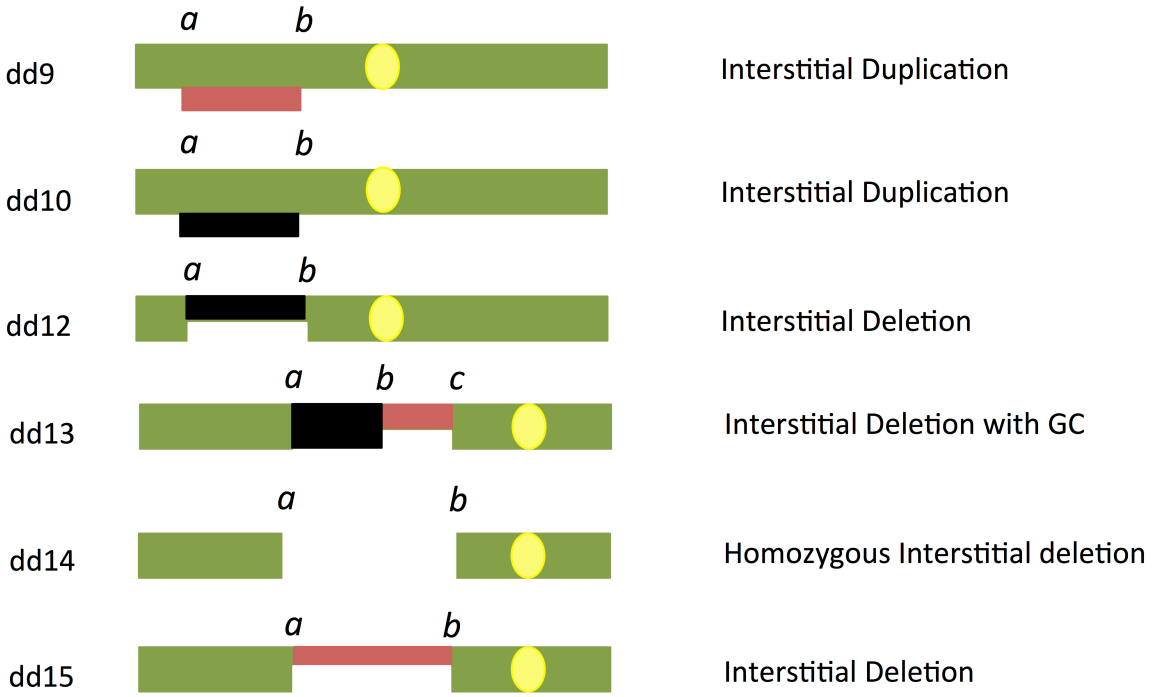

Figure S2. Deletions and duplications in sub-cultured strains. This diagram shows the patterns of deletions and duplications in diploid isolates. As in Fig. S1, the green line indicates heterozygous SNPs, and yellow circles show the centromere. The deletion or duplication is shown as line that is half as wide as the green lines. The Classes dd9 and dd10 show interstitial duplications of W303-1A-derived and YJM789-derived SNPs, respectively. The Class dd12 shows an interstitial deletion in which W303-1A-derived SNPs were removed. The coordinates for the transitions are in Table S6.

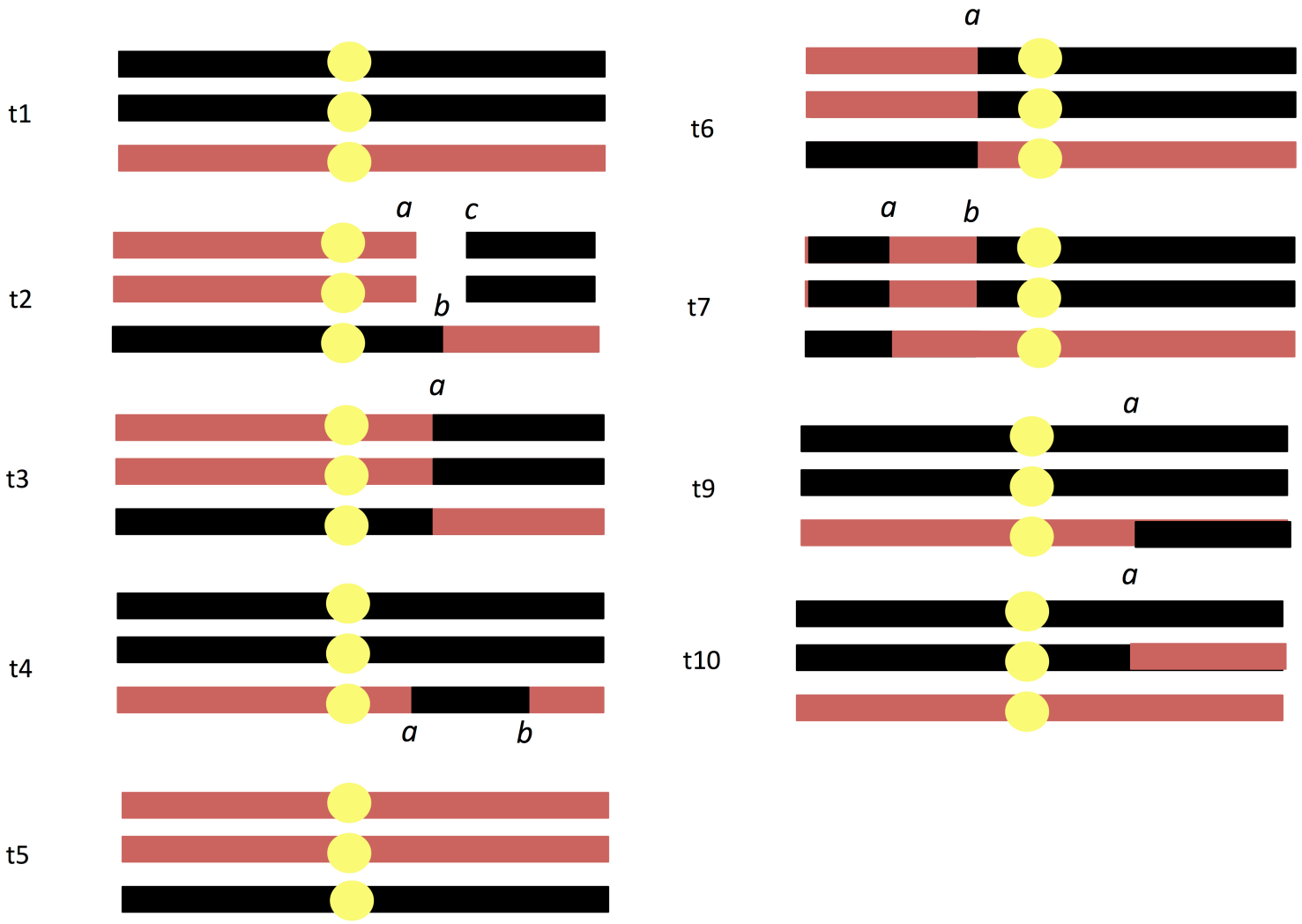

Figure S3. Aneuploidy events in sub-cultured strains. Trisomic, but not monosomic, aneuploid events were observed in our studies. For each chromosome, we indicate whether the strain has W303-1A-derived SNPs (red) or YJM789-derived SNPs (black). Note that many of these aneuploid events are associated with recombination on one or more chromosomes.

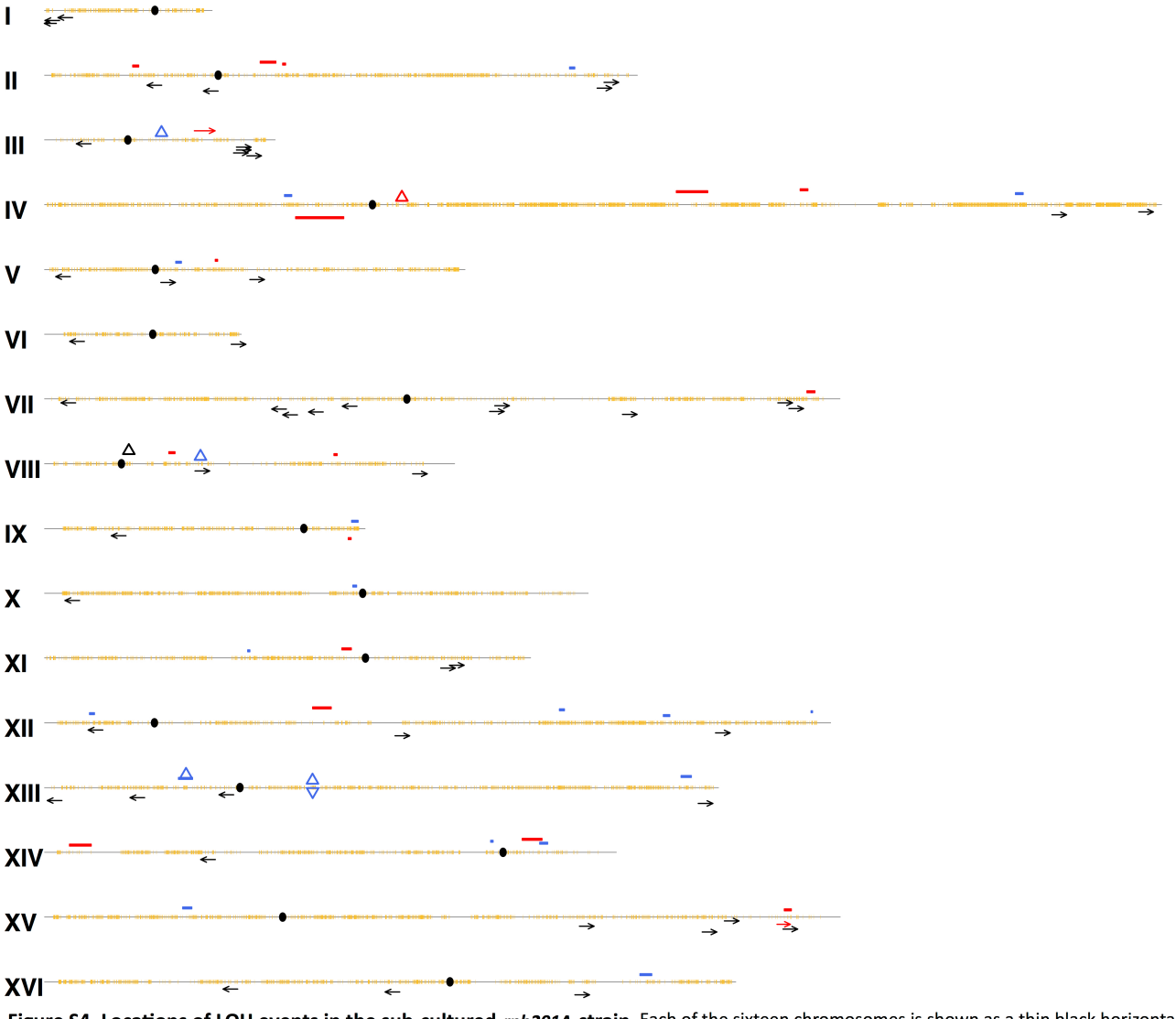

Figure S4. Locations of LOH events in the sub-cultured *rnh201Δ* strain. Each of the sixteen chromosomes is shown as a thin black horizontal line with SNPs shown as very short vertical yellow lines. The centromeres are represented by black ovals. Red and blue bars show regions of interstitial LOH in which the W303-1A-derived SNPs became homozygous and the YJM789-derived SNPs became homozygous, respectively. Black arrows indicate the positions of terminal LOH events that were unassociated with a gene conversion event. Red arrows and blue arrows indicate terminal LOH events that were associated with a conversion that made W303-1A-derived SNPs and YJM789-derived SNPs homozygous, respectively. Triangles indicate deletions (red for a deletion of W303-1A-derived sequences and blue for a deletion of YJM789-derived sequences) and inverted triangles indicate duplications (same color code as for deletions).

Figure S5. Location of LOH events in the sub-cultured *rnh1Δ rnh201Δ* strain. The mapped events are shown with the same code as Fig. S4

Figure S6. Location of LOH events in the sub-cultured *rnh201Δ pol2-M644L* strain. The mapped events are shown with the same code as in Fig. S4

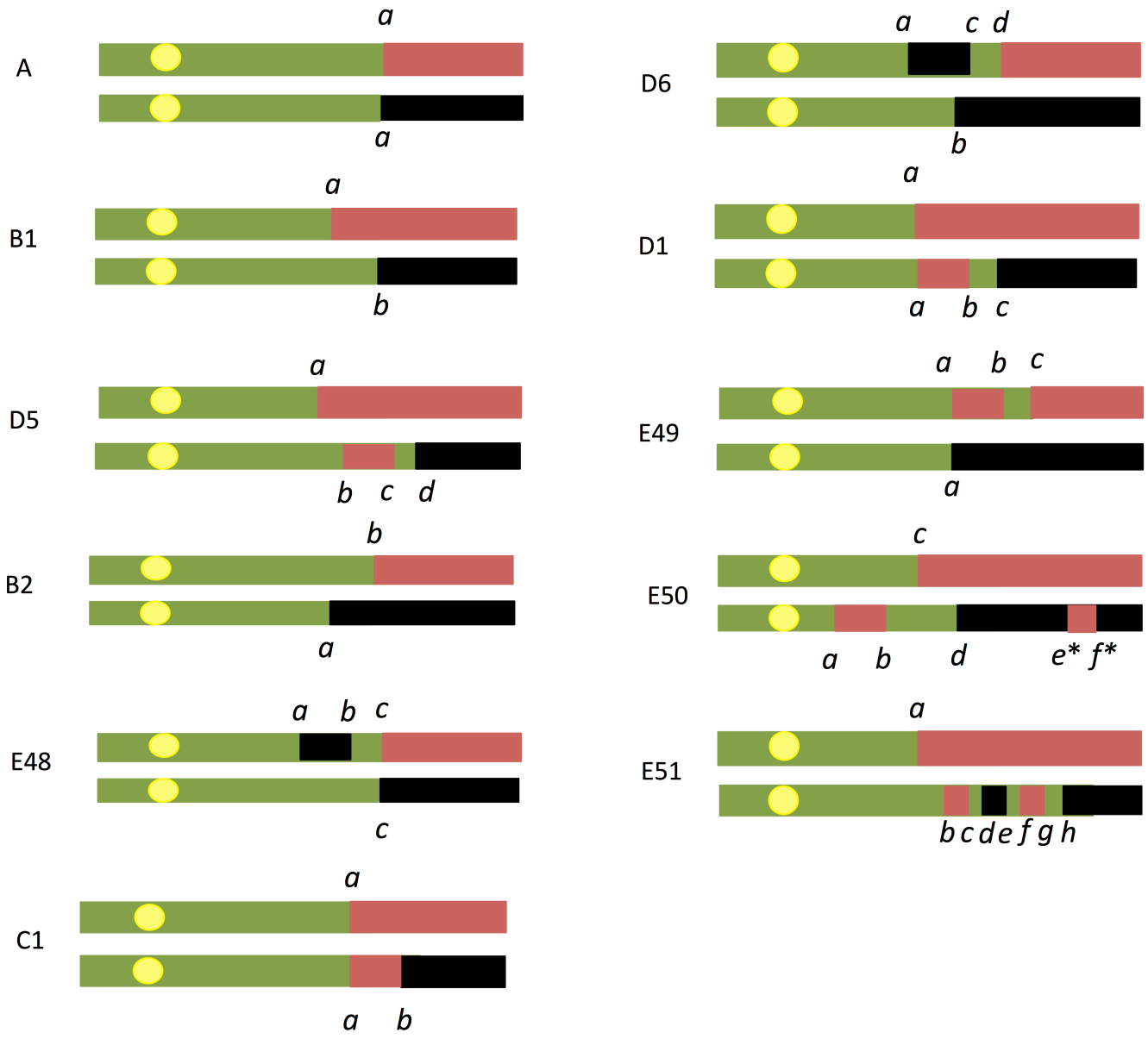

Figure S7. Patterns of LOH in sectored colonies. In this depiction, each sectored colony is represented by a pair of lines with the red sector shown as the top line. We use the same color code for heterozygous and homozygous regions as in Fig. S1. Other features of these patterns are described in the main text.